POLOIDAL MAGNETICS AND DIVERTOR STRIKE POINT CONTROL IN THE COMPACT IGNITION TOKAMAK*

D. J. Strickler, Y-K. M. Peng, and R. O. Sayer
Fusion Engineering Design Center
Oak Ridge, TN 37831

S. C. Jardin
Princeton Plasma Physics Laboratory
Princeton, NJ 08544

A. M. Rotolante
University of Florida
Gainesville, FL 32611

Abstract

The Compact Ignition Tokamak (CIT) is proposed to achieve short-pulse ignition and to study the physics of alpha-particle heating in a minimum-sized tokamak. The level of energy confinement required for ignition leads to a high-field ($B_t = 10$ T) device with a large plasma current ($I_p = 9$ MA). System studies have resulted in a baseline design with major radius $R = 1.75$ m, minor radius $a = 0.55$ m, elongation $b/a = 2.0$, and $q = 3.5$ where elongation and q are measured at the 95% flux surface. The poloidal field (PF) system for the CIT is designed for double-null divertor operation at a plasma current of $4.5\ \text{MA} \le I_p \le 9.0$ MA. Device physics specifications require that divertor operation be possible over a significant range of plasma profiles (e.g., $0.1 \le \beta_p \le 0.8$ and $0.3 \le l_i \le 0.5$) and plasma shapes (e.g., $1.6 \le b/a \le 2.0$ at $I_p = 6.3$ MA) using mainly external PF windings. Further, it should be possible to vary, in a controlled manner, the points at which the separatrix flux surface intersects the divertor plates by using some combination of external coils and internal coils of modest current. These PF system flexibility and control requirements lead to several important problems in the area of computational magnetohydrodynamic (MHD) equilibria. Specifically, methods are presented for computing free-boundary equilibria with prescribed major radius, minor radius, PF volt-seconds, and (a) divertor X-point coordinates or (b) divertor strike-point coordinates. These methods are applied in the analysis of the CIT PF system. Equilibrium solutions satisfying the above criteria yield external PF coil currents and PF coil energies that vary over a large range for the specified range of plasma profiles. A numerical optimisation technique is used to find solutions of minimum PF energy.

Introduction

In designing a divertor for an ignition tokamak,[1] it is assumed that the separatrix flux surface of the plasma meets the divertor plates at precise locations, referred to here as "strike points" (Fig. 1). The heat load on the divertor plates is sensitive to changes in location of the strike points. Original divertor designs for the CIT included shaped divertor plates (Fig. 1) and required the strike points and angle of incidence of the flux surface on the divertor plate to be very precisely controlled during a discharge. A later design concept proposes flat plates along which the inboard and outboard strike points would be continuously varied during the flattop, resulting in distribution of the heat load over a larger area. This "swept divertor" scenario is much more attractive in terms of the poloidal magnetics, and, during the time interval associated with flattop (4–6 s), a single sweep could be accomplished by using external PF coils only. These considerations impose a set of constraints on the equilibrium separatrix flux surface. Further constraints on the plasma shape include accurately positioning the outer edge of the plasma with repect to the radio frequency (RF) wave launcher and limits on the plasma scrapeoff relative to the inboard vacuum vessel.

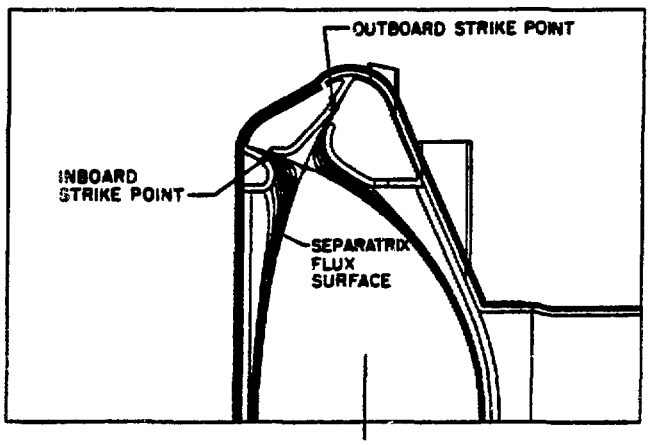

Fig. 1. CIT vacuum vessel and divertor configuration showing the strike points where the separatrix flux surface meets the divertor plates.

These requirements lead to several PF coil configuration design problems. Among these are the feasibility of using external (i.e., not linked with the TF coils) PF coils in maintaining the plasma position and strike points and the dynamic control of these parameters by using some combination of internal and external coils. In this study, we consider the first of these problems and present a numerical technique for computing coil current distributions for swept divertor scenarios and for showing, for fixed plasma shape parameters, the sensitivity of the coil currents to changes in the plasma pressure and current density profiles.

The CIT Poloidal Field System

The geometry considered here is based on a CIT design[2] with major radius $R_0 = 1.75$ m, minor radius $a = 0.55$ m, field on axis $B_t = 10.0$ T, and plasma current $I_p = 9.0$ MA. The external PF coil system is similar to that developed for the $R = 1.2$ m CIT conceptual design[3] and consists of 8 coil groups, labeled PF1 through PF8 (Table 1 and Fig. 3), that provide the equilibrium vertical field, shaping field, and inductive flux for an elongated divertor plasma. The CIT PF system design includes windings internal to the TF coils; these windings are reserved for dynamic control of shape variations caused by fast time-scale changes in plasma pressure and profiles, and they carry minimal currents.

The central solenoid stack is split into three sections (PF1, PF2, and PF3) for added flexibility in providing for a field null at startup and shaping the plasma cross section through a discharge. In this CIT design, the position and size of shaping field coil PF4 are constrained by the space reserved for a structural press on the coil's inboard side and by access for a

*Research sponsored by the Office of Fusion Energy, U.S. Department of Energy, under contract DE-AC05-84OR21400 with Martin Marietta Energy Systems, Inc.

Table 1. CIT external PF coil centers $(R_c,\ Z_c)$ and sizes $(\Delta R,\ \Delta Z)$ (m)

Coil	R_c	Z_c	ΔR	ΔZ
PF1	0.5125	0.350	0.342	0.700
PF2	0.5125	0.950	0.342	0.500
PF3	0.500	1.750	0.317	0.700
PF4	1.360	2.600	0.450	0.450
PF5	2.660	2.600	0.200	0.200
PF6	3.560	2.000	0.280	0.280
PF7	3.560	1.400	0.100	0.100
PF8	3.560	0.950	0.300	0.300

vertical diagnostic port through the plasma major radius on its outboard side. Coil PF7 is in series with the lower element of the central solenoid, PF1. The outer ring coils, PF6 and PF8, provide the major component of the vertical field, and PF6 also contributes largely to the shaping field, or higher-order derivatives of the external field. In general, all external PF coils contribute to the equilibrium, control, and shaping of the CIT plasma, as well as the flux change that induces the plasma current and ohmically heats the plasma.

Computing the Coil Current Distribution

The first problem we consider is that of using external PF coils to constrain (1) a symmetric, divertor plasma boundary to pass through two points on the midplane, $(R_0 - a, 0)$ and $(R_0 + a, 0)$, and (2) the separatrix flux surface to intersect prescribed inner and outer strike points, (R_I, Z_I) and (R_O, Z_O). The free-boundary tokamak MHD equilibrium code NEQ[4] is used in a mode in which the plasma is limited by a poloidal separatrix, and the current in one pair of coils, PF8, is adjusted to make the separatrix flux surface pass through $(R_0 + a, 0)$. The numerical software package HYBRD1[5] is used to determine the remaining free-coil currents as roots of the equation

$$\vec{F}(\vec{I}) = 0$$

where

$$\vec{F} = \begin{bmatrix} (\psi_I - \psi_x)/\Delta\psi_P \\ (\psi_O - \psi_x)/\Delta\psi_P \\ (a - a_0)/a_0 \\ (\psi_{PF} - \psi_{PF,0})/\Delta\psi_P \end{bmatrix}, \quad \vec{I} = \begin{bmatrix} I_{PF1} \\ I_{PF2} \\ I_{PF4} \\ I_{PF5} \end{bmatrix}, \qquad (1)$$

a_0 is a given plasma minor radius, ψ_I and ψ_O are the values of the poloidal magnetic flux at the inboard and outboard strike points, respectively, and $\psi_{PF} = \sum_i M_{i,P} I_i$ is the PF flux linkage with the plasma. Here $\Delta\psi_P = \psi_x - \psi_0$, where ψ_0 and ψ_x are values of the poloidal flux at the magnetic axis and separatrix, respectively, and $\psi_{PF,0}$ is a prescribed PF flux linkage with the plasma. For fixed current in coil groups PF3 and PF6 and for the given plasma profile functions, HYBRD1 calls NEQ as a subroutine to obtain values of the function $\vec{F}$ and solves for the coil currents $\vec{I}$. Typically, seven to nine equilibrium calculations are needed, with a good initial guess of the solution vector (Fig. 2). The result is a set of CIT PF coil currents $\vec{I} = (I_{PF1}, \ldots, I_{PF8})$ that satisfies the desired properties.

To solve for an equilibrium with a prescribed X point (i.e., plasma elongation and triangularity), the first two elements of the vector $\vec{F}$ [Eq. (1)] are replaced by $F_1 = (R_X - R_{X,0})/R_{X,0}$ and $F_2 = (Z_X - Z_{X,0})/Z_{X,0}$, where $R_{X,0}$ and $Z_{X,0}$ are the desired X-point coordinates.

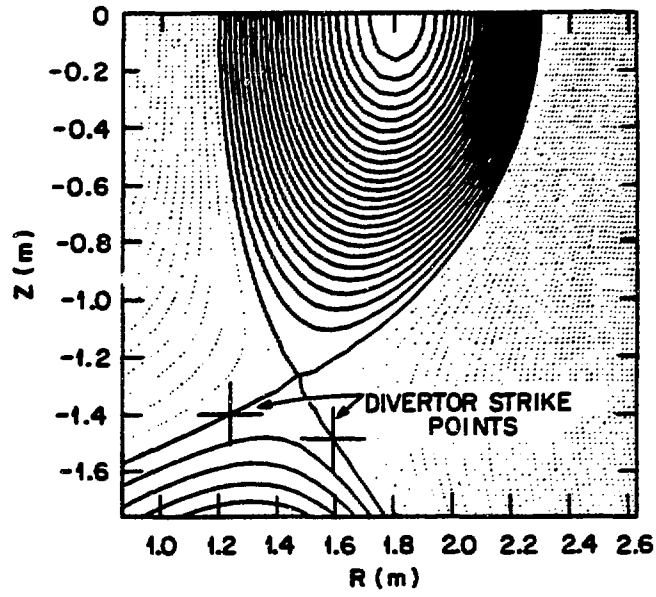

Fig. 2. Poloidal flux surfaces for a CIT equilibrium solution with prescribed major radius, minor radius, flux linkage, and divertor strike points.

A Swept Divertor Concept

For fixed plasma position, the preceding methods may be used to compute external coil current distributions consistent with the swept divertor concept. Based on PF energy considerations, a scenario where plasma triangularity increases during flattop while elongation remains relatively constant is desirable. Here the inboard strike points move from large Z to small Z while the outboard strike points move from large R to small R. Figure 3 shows one such scenario, where the inboard strike points sweep a 10-cm distance along the inboard divertor plate while the outboard strike points sweep a 20-cm distance, consistent with CIT divertor design specifications.

The coil current distributions at the start and end of the divertor sweep are given in Table 2. During the divertor sweep, the triangularity measured at the 95% flux surface increases from $\delta = 0.32$, to $\delta = 0.45$ while elongation remains at $\kappa = 2.0$. In these equilibrium calculations, the PF flux linkage has been held constant, where in a time-dependent simulation it would be increasing to match the plasma flattop volt-second requirement. This means superimposing an ohmic heating (OH) coil

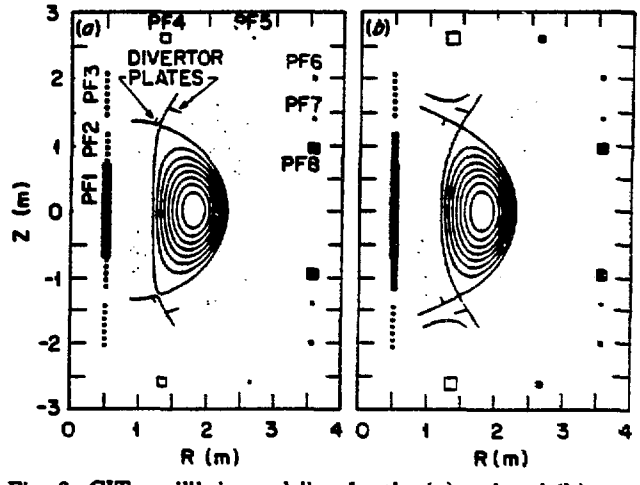

Fig. 3. CIT equilibria modeling for the (a) end and (b) start of a swept divertor scenario.

Table 2. CIT external PF coil currents at the start and end of the divertor sweep (MA)

Coil	$\bar{I}^{(start)}$	$\bar{I}^{(end)}$
PF1	13.33	15.20
PF2	2.23	−1.60
PF3	1.77	1.77
PF4	−4.62	−3.15
PF5	−0.53	0.08
PF6	0.53	0.53
PF7	0.27	0.31
PF8	4.57	4.18

current distribution for which the PF flux linkage changes while the plasma position and shape remain fixed. Note that this OH distribution can be found by using these same methods.

Effect of Profile Variations

Plasma pressure and current density profiles are characterized by the poloidal beta,

$$\beta_P = 4 \int P dV/(\mu R_0 I_P^2) , \qquad (2)$$

and the plasma internal inductance,

$$l_i/2 = \int B_p^2 dV/(\mu^2 R_0 I_P^2) , \qquad (3)$$

respectively. A nominal value for the CIT poloidal beta is $\beta_P = 0.5$, and current profiles are referred to as

$$l_i/2 = \begin{cases} 0.3 - \text{broad profile} \\ 0.4 - \text{normal profile} \\ 0.5 - \text{peaked profile} . \end{cases} \qquad (4)$$

Consider the reference CIT equilibrium of Fig. 3(b) with nominal poloidal beta and current profile. For strike points positioned for the end of flattop, the plasma parameters are given in Table 3. If the external coil current distribution is fixed at the values $\bar{I}^{(start)}$ of Table 2, the free-boundary plasma shape changes with variations in plasma pressure and current profiles, as is exhibited in Table 3 for a decrease in poloidal beta from 0.51 to 0.14.

Table 3. Free-boundary equilibrium parameters for solutions with a fixed external coil current distribution, $I_P = 9.0$ MA, $B_t = 10.0$ T, $l_i/2 = 0.4$, and a reduction in poloidal beta

		Reduced β_P
Poloidal beta	0.51	0.14
Beta (%)	2.74	0.81
Major radius (m)	1.75	1.64
Minor radius (m)	0.55	0.51
Magnetic axis (m)	1.81	1.68
$R_{X\text{-point}}$ (m)	1.46	1.38
$Z_{X\text{-point}}$ (m)	1.28	1.25
Elongation (95%)	2.00	2.09
Triangularity (95%)	0.32	0.30
Flux linkage (V-s)	22.00	20.17

The external coil current distributions were computed so as to maintain the original plasma position $R_0 = 1.75$ m, $a = 0.55$ m, inboard strike point $R_I = 1.24$ m, $Z_I = 1.40$ m, outboard strike point $R_O = 1.59$ m, $Z_O = 1.49$ m, and PF flux linkage = 22 V-s. Figure 4 shows how these coil currents vary with poloidal beta for a normal current profile. Similarly, Fig. 5 shows the dependence of the external coil current distribution on variations in the current profile for $\beta_P = 0.5$. The current in shaping coils PF2, PF4, and PF5 varies over a large range because of profile effects.

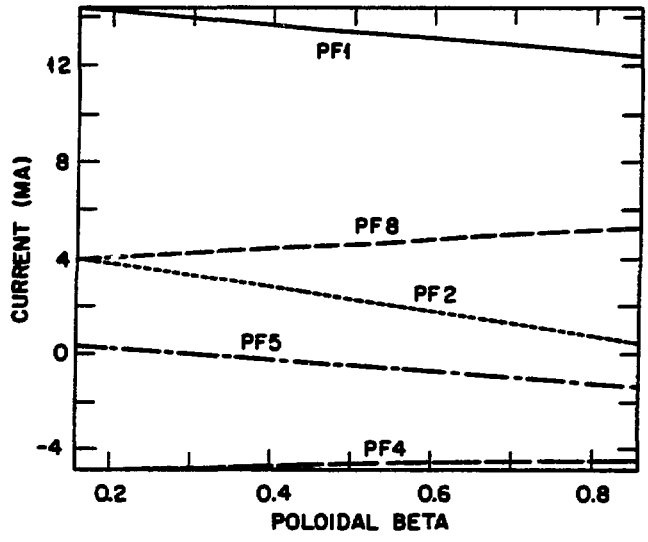

Fig. 4. Dependence of external PF coil currents on poloidal beta for prescribed plasma radii, flux linkage, and divertor strike points.

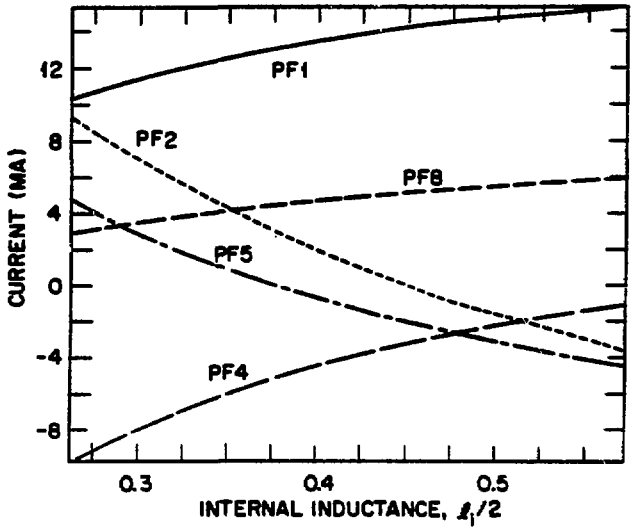

Fig. 5. Dependence of external PF coil currents on plasma current density profile for prescribed plasma radii, flux linkage, and divertor strike points.

Solutions of Minimum PF Energy

Whenever the number of variable coil currents is greater than the number of constraints, the numerical optimization package VMCON[6] is used to find the solution of minimum PF coil energy $W_{PF} = 1/2 \bar{I}^t M \bar{I}$. As an example, Fig. 6 shows the coil energy associated with the solutions of the previous section where the current profile (i.e., $l_i/2$) was varied. Also shown is a point representing a minimum PF coil energy solution in which

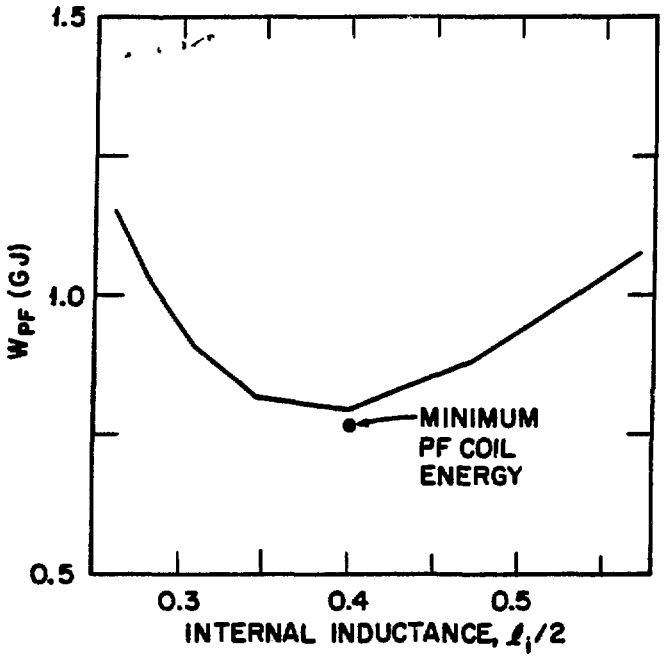

Fig. 6. Variation in PF coil energy for the external PF coil current distributions of Fig. 5 and a point representing a minimum coil energy solution for $l_i/2 = 0.4$.

the strike point locations and PF volt-seconds were treated as equality constraints but the minor radius was allowed to satisfy the inequality $|a - a_0|/a_0 < 0.015$, consistent with a physics design specification on the clearance between the separatrix flux surface and the inner wall (vacuum vessel). For this case, currents in all external coils PF1 through PF8 were treated as variables, with I_{PF8} again chosen to fix the position of the outboard edge of the plasma. For a comparable value of $l_i/2$, this solution, $\bar{I}^t$ = (11.92, 4.70, 0.91, −4.42, −0.47, 0.24, 0.65, 4.46), results in a 3% reduction in the PF energy but reduces the current in PF1 by 1.4 MA, which is important in terms of solenoid temperature and stress limits.

Conclusions

Methods are presented for computing free-boundary MHD equilibria with prescribed constraints on plasma position, PF volt-seconds, and divertor strike-point or X-point coordinates. These methods are used to show the feasibility of using external PF coils to position and shape the plasma flux surfaces relative to the divertor plates in the CIT and to present a scenario for a swept divertor.

Forcing the separatrix flux surface to coincide with four prescribed points in the poloidal plane, over some range of uncertainty in plasma pressure and current profiles, requires four relatively independent coil groups. The degree of independence in these coil groups is often limited by physical constraints on their locations, which can result in large variations in coil currents because of profile uncertainty.

References

[1] R. Gallix, "CIT Divertor Plate Profile Study," GA Technologies memo B-861204-G-01 (December 1986).

[2] J. Schmidt et al., "A Compact Ignition Experiment," to be published in *Proceedings of the 11th International Conference on Plasma Physics and Controlled Nuclear Fusion Research (Kyoto, Japan, November 1986).*

[3] R. J. Thome et al., *Poloidal Field Coil System Design for the Compact Ignition Tokamak (CIT)*, MIT Plasma Fusion Center Report PFC/RR-86-11 (April 1986).

[4] D. J. Strickler, J. B. Miller, K. E. Rothe, and Y-K. M. Peng, *Equilibrium Modeling of the TFCX Poloidal Field Coil System*, ORNL/FEDC-83/10 (April 1984).

[5] J. J. Moré, B. S. Garbow, and K. E. Hillstrom, *User Guide for MINPACK-1*, Argonne National Laboratory Report ANL-80-74 (1980).

[6] D. Crane, K. Hillstran, and M. Minkoff, *Solutions of Nonlinear Programming Problem with Subroutine VMCON*, Argonne National Laboratory Report ANL-80-64 (1980).

DISCLAIMER